TWO NOVEL MEMS ACTUATOR SYSTEMS FOR SELF-ALIGNED INTEGRATED 3D OPTICAL COHERENT TOMOGRAPHY SCANNERS

Aleksandar Jovic[1], Gregory Pandraud[1], Nuria Sanchez[2], Juan Sancho[2], Kirill Zinoviev[3], Jose L. Rubio[2], Eduardo Margallo[2] and Pasqualina M. Sarro[1]
[1]Delft University of Technology, Delft, THE NETHERLANDS
[2]MedLumics, SL., Madrid, SPAIN
[3]IMEC, Leuven, BELGIUM

ABSTRACT

Two novel MEMS actuator systems (a torsional one and a deflecting one) for a new self-aligned integrated 3D optical coherent tomography (OCT) scanner are reported. These new systems, with a footprint of 2.5mm×2.5 mm each, provide a *x* and *y* scanning range of 730 µm (tilting range of 8°) with an average power consumption of 150 mW. As the device integrates a silicon collimating micro lens, an optical waveguide and a MEMS actuator system on a single chip, it provides a considerable decrease in optical losses thanks to the intrinsic alignment obtained during fabrication, while significantly reducing the complexity and time that assembly and packaging of separate components demand, therefore making fully integrated, miniaturized 3D OCT scanners feasible.

INTRODUCTION

A successful treatment of melanoma, a disease with a significant incidence increase in the past decades, strongly depends on early detection [1]. In general, examination is done by a standard biopsy procedure, which involves actual skin tissue removal and requires to be performed by medical specialists. Contrary to standard methods, optical coherence tomography (OCT) relies on noninvasive *in vivo* medical imaging. Typically, it uses near infrared light to generate 3D images of live morphology of biological tissues, up to 3 mm depth [2].

The OCT scanners are low coherent interferometers. An image is generated by measuring the difference in optical path of the reference and the scattered beams. Up to now, the technique was mainly developed using optical fiber based devices. The introduction of MEMS micro mirrors has made miniaturization of these scanners possible and finally, through the reduction in size and price and the packaging in probes, portable [3].

Ever since, state of the art OCT systems consist of several discrete elements such as photonic circuitry (optical fibers, beam splitters etc.), a separate collimating lens and MEMS micro mirrors [3,4], as schematically depicted in Fig. 1. As any other interferometer, the OCT requires good optical alignment of the discrete components within the package. Hence, quality of the image still depends on complicated and time-consuming aligning, assembly and packaging procedures [5].

Consequently, research in this field focused on simplifying assembly [6], improving signal acquisition [7], and especially on improving the motion range of MEMS mirrors for larger area scanning [3]. However, the main problem of time consuming optical alignment of discrete components remains unsolved.

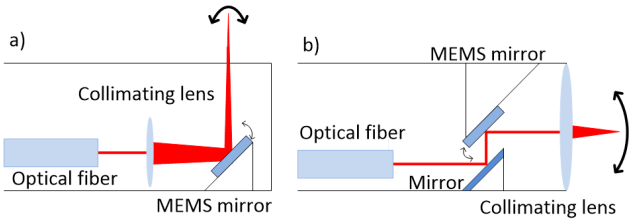

Figure 1: Schematics for the state of the art MEMS based OCT probes. (a) Side-view probe (b) Forward-view probe assembled from several discrete components.

In this paper, we present the integration of all scanner components within a single MEMS device where optical fibers are replaced by a Si photonic integrated circuit, a collimated Si micro lens and a scanning mirror with a novel actuator system. This new solution provides optical self-alignment during fabrication. Moreover, complexity is significantly reduced, assembly is simplified and most importantly, optical losses are reduced. In addition, this concept solves the compatibility issue related to the different fabrication technologies discrete components require.

As first step towards the proposed concept, the main components, i.e. photonic circuit, Si micro lens and MEMS actuator system, are fabricated and optimized individually. Each of the components is designed to be compatible with rest of the system. Also, the process flow for each building block is embedded in the flow defined for the integrated system.

This paper focuses on the MEMS actuator system, which is the most challenging part to design and fabricate. The concept of this novel self-aligned integrated OCT scanner is presented and the system design explained. Next, the main fabrication steps for the MEMS actuator system are described. Finally, characterization of the fabricated devices is presented.

SELFT-ALIGNED INTEGRADTED 3D OCT SCANNER DESIGN

To obtain 3D OCT images, optical surface scanning is needed. This translates in 2D motion of the scanning system. Fig. 2 depicts the two new concepts for lateral scanning, in which a Si waveguide replaces the optical fiber. For the OCT systems that operate with a center wavelength of 1300nm, Si can be used for both lens and waveguide fabrication, thus making the presented designs a fully integrated MEMS optical scanner.

The device shown in Fig. 2a provides horizontal scanning (*x* direction) by tilting the lens, located at the bottom of the moving plate, around torsional hinges. The

structure in Fig. 2b provides scanning of the bulk microplate (*y* direction) by out-of-plane deflection of a supportive hinge. In both cases, the light signal travels through a Si waveguide which runs over the hinge and ends up with a 45° mirror facet. The optical signal scatters into the bulk Si microplate and exits through the collimated lens at the bottom of the plate. Combination of these two systems will provide 2D surface scanning, i.e. 3D OCT image.

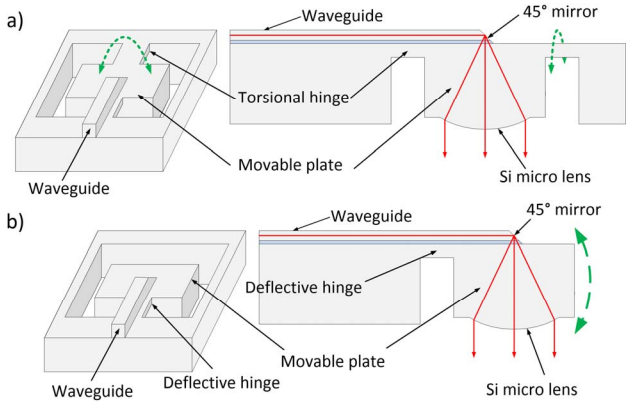

Figure 2: The novel fully integrated OCT scanning concept with tilting micro lens supported with (a) torsional hinges (b) deflecting hinge.

The Al-SiO_2 electrothermal bimorph cantilevers can generate high out of plane displacement but they are slow [8]. However, this is not an issue here as the desired working speed of this novel OCT scanner is 10 Hz. The SOI device layer is used for low loss (0.13 dB) waveguide fabrication [9], while hinges are made from bulk silicon. The micro lens is a Si spherical lens with roughness of only 25nm [10], which is much lower than λ/10, thus satisfying the demanding OCT optical requirements. SEM images of a part of a fabricated photonic circuit and a Si micro lens are shown in Fig. 3

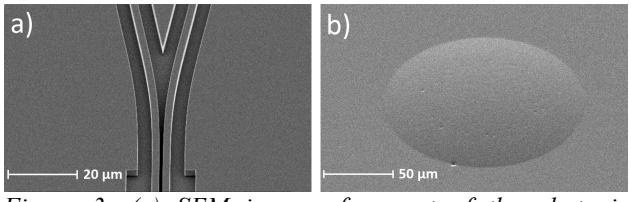

Figure 3: (a) SEM image of a part of the photonic integrated circuit fabricated based on the process reported in [9] (b) SEM image of the Si micro lens [10].

The proposed fully integrated OCT scanner is schematically given in Figs.4 and 5. The torsional based device, shown in Fig. 4a has 4 electro-thermal Al-SiO_2 bimorph actuators on each side of the bulk microplate. Actuators are 500 µm long and 110 µm wide with 2 µm thick Al as bottom layer and 2 µm thick SiO_2 as top layer of the bimorph. Both sets of actuators are pre-stressed and pushing the microplate (800 µm × 800 µm) down. Once power is supplied to one group of actuators they will release the pressure from the plate. When the plate is pressed only on one side, rotation around the hinge (*x* direction) is created. This working principle is illustrated in Fig. 4b. Torsional hinges are 10 µm thick and 500 µm long.

The deflecting based device is illustrated in Fig. 5a. It consists of a bulk microplate (1 mm × 450 µm), which is suspended with a hinge of 10 µm height, 50 µm width and 800 µm length. The hinge is deflected using 4 electro thermal Al-SiO_2 bimorph actuators, each 800 µm long and 110 µm wide. Bimorph layer order and thickness are the same as for the torsional based device. The bimorph cantilevers are pre-stressed and deflected. Since the microplate is suspended only on one side, the hinge is also deflected, resulting in an initial angular displacement of the plate. Actuation of the bimorphs will result in out of plane motion, hence rotating the plate around the axis in the *y* direction (Fig. 5b).

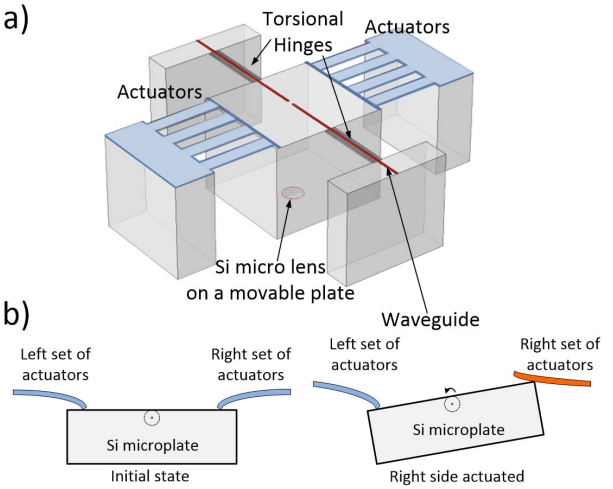

Figure 4: (a) 3D model (b) Working principle of the novel torsional hinge based OCT scanning systems.

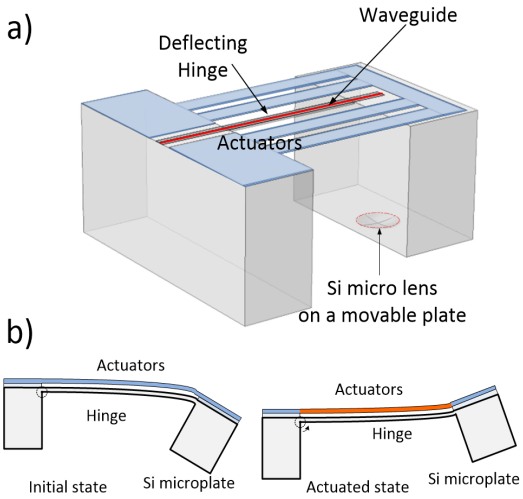

Figure 5: (a) 3D model (b) Working principle of the novel deflecting hinge based OCT scanning system.

Both systems have the same hinge height and the same bimorph layer thicknesses and consequently, they can be fabricated together. The rotational axes for both devices are perpendicular to each other. Combining these two devices into one will produce a system with 2 degrees of freedom which is needed for 2D surface scanning, i.e. for 3D OCT imaging.

FABRICATION PROCESS

For the new OCT scanner fabrication, SOI wafers are needed. The top silicon layer is used for the waveguide fabrication, while the hinges and the lens are realized in the bulk silicon and the bimorph actuators are added on at the surface. However, for the actuators optimization, bare silicon wafers are used, but to preserve integration, the process is designed to be compatible with the previously developed fabrication flows for the photonic circuitry [9] and the micro lens [10].

First, 3 µm thick sacrificial layer of plasma enhanced chemical vapor deposition (PECVD) SiO_2 is deposited. Next, 300 nm of Al is sputtered and patterned to define the heater (Fig. 6a). For electrical insulation between heater and bimorph layer, 100 nm of Al_2O_3 is added using atomic layer deposition (ALD). Next, 2 µm of sputtered Al and 2 µm of PECVD SiO_2 are deposited to form the bimorph (Fig. 6b). The SiO_2 layer is patterned and encapsulated with 200 nm of ALD Al_2O_3 to protect it during the vapor HF release (Fig. 6c). Patterning of the Al layer (Fig. 6d) completes the actuators definition. The hinges are pre-defined using a 10-15 µm deep reactive ion etching (DRIE) after which PECVD SiO_2 is added as a stop layer (Fig. 6e) for the two-step DRIE from the wafer backside (Fig.6f and Fig 6g). Finally, the device is released by removing both SiO_2 sacrificial and stop layers using vapor HF, while the SiO_2 bimorph layer is preserved due to the ALD alumina protection. In Fig. 7 SEM and optical images of the fabricated devices are shown.

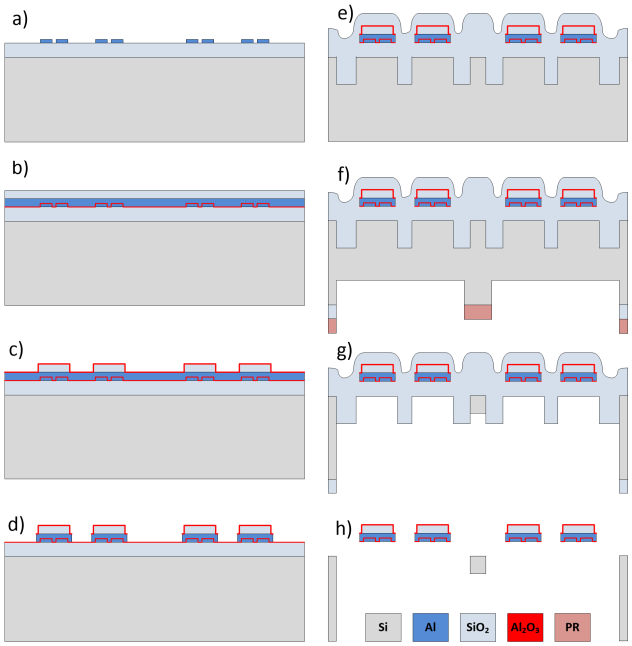

Figure 6: Main steps of the fabrication process for the MEMS actuator systems: (a) Sacrificial SiO_2 layer deposition and Al heater definition; (b) Al_2O_3 electrical insulation layer deposition followed by 2 µm Al and 2 µm SiO_2 bimorph layer deposition; (c) SiO_2 layer patterning and Al_2O_3 deposition for vapor HF protection; (d) Al layer patterning; (e) Top side Si hinge definition and stop layer deposition; (f) First backside DRIE; (e) Second backside DRIE; (f) Vapor HF device release.

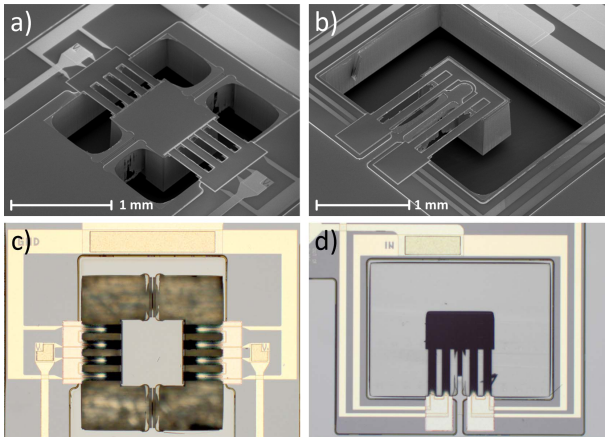

Figure 7: SEM images of (a) torsional hinge based and (b) deflecting hinge based MEMS actuator system before final release. Optical image of packaged device: (c) torsional hinge based (d) deflecting hinge based system.

DEVICE CHARACTERISATION

To evaluate the MEMS actuator systems performance, static measurement of angular displacement versus input power is done. First, using white light interferometer (WLI), out of plane displacement of the microplate is measured for both devices, while electrical power was supplied to the actuators. The displacements are measured on two edge points of the microplate. Considering the horizontal distance of the measurement points, torsion/deflection angle is calculated. This principle is illustrated in Fig. 8

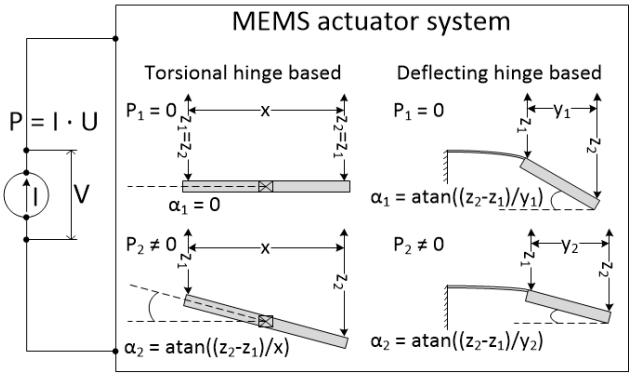

Figure 8: Angular displacement measurement principle for (a) torsional hinge and (b) deflecting hinge based MEMS actuator system.

In Fig. 9 measurement results of angular displacement versus input power for both MEMS actuator systems are reported. A tilting range of 8° with an average power consumption of 150 mW is measured for both devices, which satisfies the range of 730µm×730µm surface scan for OCT skin imaging. Measurements are repeated (1000 cycles for torsional hinge and 5000 cycles for deflecting hinge) and almost no deterioration of the system performance was observed. The angular tilt shows linear dependence on the input power for torsional hinge based device for the full range of 8° (Fig. 9a) which can significantly simplify the control of the scanner.

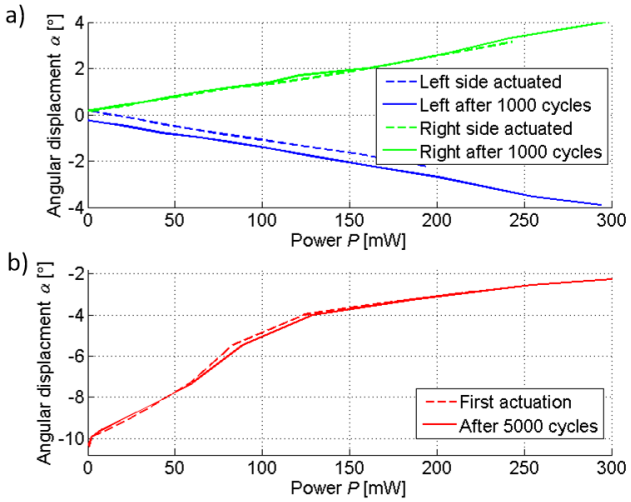

Figure 9: Measured angular displacement versus input power for (a) torsional hinge based (b) deflecting hinge based MEMS actuator systems.

The frequency response of the actuator systems is measured in the range 50 Hz - 4 kHz using a Laser Doppler Vibrometer (LDV) and the results are displayed in Fig. 10. The torsional hinge based device has the first resonant mode at 678 Hz and the second at 2267 Hz (Fig. 10a) while the defecting hinge based device has modes at 297 Hz and 1976 Hz. Both systems have more than 10-time higher resonant frequency compared to the desired working speed of 10 Hz.

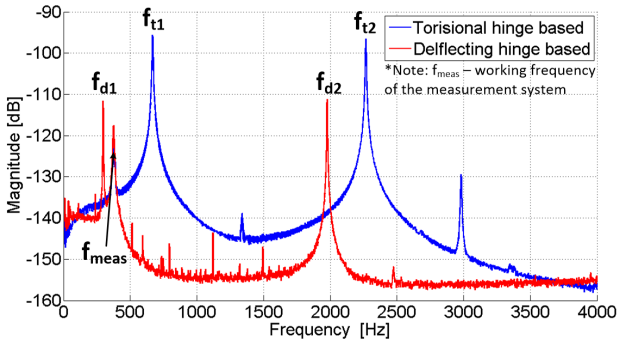

Figure 10: Frequency response of torsional hinge (blue) and deflecting hinge (red) based MEMS actuator systems.

CONCLUSION

We presented two novel MEMS actuators systems for a self-aligned integrated OCT scanner. Both systems provide the desired tilting range of 8° with an average power consumption of 150 mW showing stable performance over time. Also, their resonant frequencies are much higher than the desired scanning speed of 10 Hz. Further optimization of the actuator system will result in a higher motion range. Next step will be to combine the already tested process for waveguide and lens fabrication with the developed new MEMS actuator system, so to fabricate all components in one integrated device.

The proposed integrated design is meant to replace the current state of the art MEMS based OCT scanners, as it provides the required performance while self-alignment during fabrication drastically simplifies device assembly and packaging.

ACKNOWLEDGEMENTS

The work presented in this paper is part of the BiopsyPen project, 7th Framework Programme of European Commission under grant agreement nº 611132. The help of the Else Kooi Laboratory (previously DIMES) staff of TU Delft is greatly appreciated. Special thanks go to B. Morana, J. Wei and M. R. Venkatesh from TU Delft for fabrication and measurement advices. Also, we are grateful to R. Sanders from Micro Sensors and Systems group of University of Twente for his help during dynamic characterization of the actuator system.

REFERENCES

[1] J. A. Usher-Smith, J. Emerly, A. P. Kassianos and F. M. Walter, "Risk Prediction Models for Melanoma: A Systematic Review", *Cancer Epidemiology, Biomarkers & Prevention*, Vol. 23, Iss. 8, pp. 1450-1463, 2014

[2] W. Drexler, "Ultrahigh-resolution optical coherence tomography", *Journal of Biomedical Optics*, Vol. 9, Iss. 1, pp 47-74, 2004

[3] J. Sun and H. Xie, "MEMS-Based Endoscopic Optical Coherence Tomography", *International Journal of Optics*, Vol. 2011, 825629, 2011.

[4] K. Jia, S. Pal and H. Xie, "An Electrothermal Tip–Tilt–Piston Micromirror Based on Folded Dual S-Shaped Bimorphs", *Journal of Microelectromechanical* systems, Vol. 18, No. 5, pp. 1004-1015, October 2009.

[5] S.H. Lee and Y.C. Lee, "Optoelectronic packaging for optical interconnects", *Optics and photonics news*, Vol. 17, Iss. 12, pp. 40-45, 2006.

[6] Y. Xu, J. Singh, C. S. Premachandran, A. Khairyanto, K. W. S. Chen, N. Chen, C. J. R. Sheppard and M. Olivo, "Design and development of a 3D scanning MEMS OCT probe using a novel SiOB package assembly." *Journal of Micromechanics and Microengineering*, Vol. 18, 125005, 2008.

[7] P. Guerra, J.J. Valverde, A. Martin, M.J. Ledesma, J.L. Rubio and A. Santos, "Real Time Signal Processing and Data Handling with dedicated hardware in handheld OCT Device", *Journal of Instrumentation*, Vol. 10, C11001, 2015.

[8] D. J. Bell, T. J. Lu, N. A. Fleck and S. M. Spearing, "MEMS actuators and sensors: observations on their performance and selection for purpose", *Journal of Micromechanics and Microengineering*, Vol. 15, pp. S153–S164, 2005.

[9] K. Solehmainen, T. Alto, J. Dekker, M. Kapulainen, M. Harjanne, K.Kukli, P. Heimala, K. Kolari and M. Leskela, "Dry-Etched Silicon-on-Insulator Waveguides With Low Propagation and Fiber-Coupling Losses", *Journal of Lightwave Technology*, Vol. 23, No. 11, pp 3875-3880, 2005.

[10] A. Jovic, G. Pandraud, K. Zinoviev, J. L. Rubio, E. Margallo, P. M. Sarro, "Fabrication process of Si microlenses for OCT systems", *Proc. SPIE 9888*, Micro-Optics, 98880C, 2016

CONTACT

*A. Jovic, tel: +31-6-15342385; a.jovic@tudelft.nl